

Variational Auto-Decoder: Neural Generative Modeling from Partial Data

Amir Zadeh¹ Yao-Chong Lim² Paul Pu Liang³ Louis-Philippe Morency¹

Abstract

Learning a generative model from partial data (data with missingness) is a challenging area of machine learning research. We study a specific implementation of the Auto-Encoding Variational Bayes (AVEB) algorithm, named in this paper as a Variational Auto-Decoder (VAD). VAD is a generic framework which uses Variational Bayes and Markov Chain Monte Carlo (MCMC) methods to learn a generative model from partial data. The main distinction between VAD and Variational Auto-Encoder (VAE) is the encoder component, as VAD does not have one. Using a proposed efficient inference method from a multivariate Gaussian approximate posterior, VAD models allow inference to be performed via simple gradient ascent rather than MCMC sampling from a probabilistic decoder. This technique reduces the inference computational cost, allows for using more complex optimization techniques during latent space inference (which are shown to be crucial due to a high degree of freedom in the VAD latent space), and keeps the framework simple to implement. Through extensive experiments over several datasets and different missing ratios, we show that encoders cannot efficiently marginalize the input volatility caused by imputed missing values. We study multimodal datasets in this paper, which is a particular area of impact for VAD models.

1. Introduction

In many naturally occurring scenarios, the input data may not be fully observable. This in turn leads to the presence of missing information where only partial data is observable. As one example, when studying an object, the entire geometrical surface may not be fully observable from a monocular

¹Language Technologies Institute, Carnegie Mellon University ²School of Computer Science, Carnegie Mellon University

³Machine Learning Department, Carnegie Mellon University. Correspondence to: Amir Zadeh <abagherz@cs.cmu.edu>.

camera due to self occlusions. Learning from partial data is a challenging area of machine learning, especially in generative modeling, where the goal is to create a probabilistic space for the data. In the area of generative modeling, partial data poses a cyclic challenge: to replace the missing information (statistical imputation), one needs to know the underlying generative distribution of the data; and to learn the underlying generative distribution, one needs to know the missing information. To break this cycle, a trivial heuristic is to assume a simple generative distribution for the data.

Common statistical imputation techniques are developed based on this heuristic such as imputation with constants (zero or mean imputation) or model-based imputations based on assuming known distributions for the data (e.g. Gaussian Mixture Models). Aside from being easy to implement, a particular appeal of these simple techniques is that they allow for subsequent use of well-known generative and unsupervised models which commonly use an encoder to learn a representation space. Naturally, as the missingness becomes more complex, the encoder is assumed to be able to marginalize the effect of approximate imputations, thus remaining consistent in generating a meaningful representation space.

An alternative approach in dealing with the above cycle is to not replace the missing values, and use Variational Bayes and Markov Chain Monte Carlo (MCMC) techniques to learn a probabilistic generative space for partial data. In doing so, an approximate posterior for the latent space is assumed, and training is performed until decoded samples from the approximate posterior match the likelihood of the input data. This approach falls within the formulation of Auto-Encoding Variational Bayes (AEVB) algorithm (Kingma and Welling, 2013). AEVB is commonly implemented using variants of Variational Auto-Encoders (VAE (Kingma and Welling, 2013)), where the approximate posterior for the latent space is derived by an encoder.

In this paper, we outline the Variational Auto-Decoder (VAD) model, where no encoder is used during AVEB learning process. We present an efficient implementation of VAD models based on the widely adopted assumption that the approximate posterior for data points follows a multivariate normal distribution. Our experiments demonstrate the superior performance of VAD in dealing with partial data

compared to VAE, which shows that expecting a generic encoder to marginalize the effect of missing (or imputed) dimensions is not practically justified. Beyond superior performance in modeling partial data, VAD models also demonstrate outstanding performance in adversarial environments where train and test missingness distributions are different.

2. Background

In this section we outline the required background for the studies in this paper.

Maximum Likelihood Estimation

Consider a given dataset $X = \{x_1, \dots, x_N\}$ with N data-points, each sampled i.i.d. from a distribution $p(x)$. The parameters θ of a probabilistic model can be learned by maximizing the likelihood $p(X|\theta)$, w.r.t θ . In practice often the log of the likelihood is calculated and used:

$$\mathcal{L}(\theta|X) = \sum_{i=1}^N \log p(x_i|\theta) \quad (1)$$

Variational Bayes Methods

For any given datapoint x_i and any approximate posterior distribution $q(z|x_i, \phi)$ with z as an unobserved random variable and ϕ as parameters of q , we can rewrite the likelihood terms $\mathcal{L}(\theta|x_i) = \log p(x_i|\theta)$ as follows:

$$\begin{aligned} \mathcal{L}(\theta|x_i) &= \int \log p(z, x_i|\theta) dz \\ &= - \int q(z|x_i, \phi) \log \frac{p(z|x_i, \theta)}{q(z|x_i, \phi)} dz \\ &\quad + \int q(z|x_i, \phi) \log \frac{p(z|x_i, \theta)p(x_i|\theta)}{q(z|x_i, \phi)} dz \end{aligned} \quad (2)$$

with the condition that $q(z|x_i, \phi) > 0$ if $p(z|x_i, \theta) > 0$. To simplify notation, we refer to posterior $p(z|x_i, \theta)$ as $p_\theta(z|x_i)$ and approximate posterior $q(z|x_i, \phi)$ as $q_\phi(z|x_i)$. More simply, the likelihood in Equation 2 can be written as:

$$\mathcal{L}(\theta|x_i) = \text{KL}(q_\phi(z|x_i) \parallel p_\theta(z|x_i)) + \mathcal{V}(q_\phi, \theta|x_i) \quad (3)$$

In the above equation, KL is the Kullback—Leibler divergence. \mathcal{V} is the variational lower-bound of the log-likelihood, which is equal to sum of the expected value of the log of the posterior $p_\theta(z|x_i)$ under distribution $q_\phi(z|x_i)$ and entropy of q :

$$\mathcal{V}(q_\phi, \theta|x_i) = \mathbb{E}_{q_\phi(z|x_i)} [\log p_\theta(z, x_i) - \log q_\phi(z|x_i)] \quad (4)$$

Through the above formulation, rather than employing a method for learning model parameters through likelihood of

data, Variational Bayes methods approximate the posterior probability $p_\theta(z|x_i)$ with a simpler distribution $q(z|x_i)$.

Markov Chain Monte Carlo Methods (MCMC)

If the posterior $p_\theta(z|x_i)$ is not easy to sample from, an iterative random walk approach can be taken to sample from it. A notable approach for this purpose is the Metropolis-Hastings algorithm (Metropolis *et al.*, 1953). In a neural generative modeling framework, sampling from a decoder w.r.t to its input is not trivial (since non-linear neural network decoders are generally not easily invertible).

3. Problem Formulation

We assume a ground truth random variable $\hat{x} \sim p(\hat{x})$; $\hat{x} \in \mathbb{R}^d$, sampled from a ground truth distribution, d being the dimension of the input space. Unfortunately, the space of \hat{x} is not fully observable due to a certain phenomena. The part that is observable we denote via random variable x , regarded hereon as partial input. We assume that a random variable $\alpha \sim p(\alpha|\hat{x})$; $\alpha \in \{0, 1\}^d$ denotes whether or not the data is observable through an indicator in each dimension with value 1 being observable and 0 being missing. α is regarded as the missingness pattern hereon.

We formalize the process of generating the random variable x as the process of first drawing a ground-truth data sample from $p(\hat{x})$ and a missingness pattern sample from $p(\alpha|\hat{x})$, and subsequently removing information from \hat{x} using α . We draw N samples from the above process to build a dataset¹. The partial dataset is regarded as $X = \{x_1, \dots, x_N\}$ and the missingness patterns are regarded as $A = \{\alpha_1, \dots, \alpha_N\}$. The ground-truth dataset is regarded as $\hat{X} = \{\hat{x}_1, \dots, \hat{x}_N\}$ (which is known only to an oracle, hence never a part of training, validation or testing). We consider a differentiable parametric function $\mathcal{F}(\cdot; \theta) : z \mapsto x$ as a decoder to be a mapping between an unobserved latent variable $z \sim p(z|x)$; $z \in \mathbb{R}^{d_z}$ and x (d_z is the dimension of posterior space). \mathcal{F} can be a large class of parametric models including layered neural networks with well-known operations including affine mappings, convolutions, activation functions, etc.

4. Variational Auto-Decoder (VAD)

Contrary to the common VAE implementation of AVEB which uses a probabilistic encoder to derive $q_\phi(z|x_i)$, VAD derives the same approximate posterior without an encoder. This in turn makes the inference (or forward pass) a major distinction between the two. We first outline a generic inference and training framework for VAD models using Variational Bayes and Markov Chain Monte Carlo (MCMC)

¹Notably, each datapoint can have a distinct missingness pattern.

approaches. Afterwards we discuss an alternative efficient implementation of the inference process which simplifies sampling from the decoder for the choice of a normal distribution as the approximate posterior.

4.1. Inference and Training

The inference step is the major distinction between VAD and VAE models. Hence, we first start by discussing the inference procedure and subsequently discuss the training procedure.

4.1.1. INFERENCE

During the proposed inference approach, we assume that a trained decoder $\mathcal{F}(z|\theta^*)$ is provided (with trained parameters θ^* , the actual optimization of θ is discussed in the next Subsection). Using this trained decoder and individual samples $x_i \in X$, we define the below posterior distribution:

$$p(z|x_i, \Lambda_i) = \mathcal{N}(\mathcal{F}(z; \theta^*); x_i, \Lambda_i) \quad (5)$$

This density is built based on probabilistically inverting the decoder $\mathcal{F}(z|\theta^*)$ using a normal distribution centered at the given data point x_i . The covariance Λ_i is defined as a diagonal positive semi-definite matrix with α_i on its main diagonal whenever $\alpha_i \neq 0$. The missing dimensions are simply removed by marginalization.

Sampling z using the above posterior can be done using Metropolis-Hastings algorithm (Metropolis *et al.*, 1953). Given z_t , the sample drawn at time t , we define the probability $z \sim g(z|z_t) = \mathcal{N}(z; z_t, \Sigma_g)$ based on the symmetric proposal density $g(z|z_t)$. In other words, the possible steps to be taken at time $t+1$ follow a normal distribution centered around z_t . Therefore, points closer to z_t are more likely to be visited next and this makes the sequence of samples resemble a random walk when sampling from the posterior $p(z|x_i, \Lambda_i)$. Σ_g controls the distance of the steps in the random walk. The following acceptance criteria is defined based on the output of the posterior $p(z|x_i, \Lambda_i)$:

$$c = \min \left(\frac{p(z_{t+1}|x_i, \Lambda_i)}{p(z_t|x_i, \Lambda_i)}, 1 \right) \quad (6)$$

At time t , a sample is drawn from the trial Bernoulli(c), with c being the probability of outcome of 1. If the outcome of the trial is 1, then the step is accepted, if the outcome is 0, the step is rejected and $z_{t+1} = z_t$. This is iteratively performed until a certain number of samples are reached. The output of this sampling process is a set of points $Z = \{z_1, \dots, z_T\}$ with T the number of samples drawn from posterior $p(z|x_i, \Lambda_i)$.

In a Variational Bayes framework, an approximate posterior $q(z|x_i)$ is employed to generate similar density and samples as $p(z|x_i, \Lambda_i)$. Unlike the posterior $p(z|x_i, \Lambda_i)$, q is chosen

Algorithm 1 Inference process for the VAD models with multivariate normal distribution as approximate posterior.

```

1:  $q : \{\mu_i^{(0)}, \Sigma_i^{(0)}\} \leftarrow \{\mathcal{U}(-\epsilon, \epsilon), I_\epsilon\}$        $\triangleright$  init w.  $\epsilon \approx 0$ 
2: repeat:
3:    $[z] \sim q(z|x_i; \mu_i^{(t)}, \Sigma_i)$        $\triangleright$  Monte-Carlo sampling
4:    $[p(z|x_i, \theta^*)] = \mathcal{N}(\mathcal{F}([z], \theta^*); x_i, \Lambda_i)$        $\triangleright$  Eq. 5
5:    $\{\mu_i, \Sigma_i\}^{(t+1)} \leftarrow \text{grad\_step}_{\mu_i, \Sigma_i} \left( \mathcal{V}(q^{(t)}, \theta^*|x_i) \right)$ 
6:    $t \leftarrow t + 1$ 
7: until convergence on  $\mathcal{V}$ 

```

Algorithm 2 Training process for the VAD models with multivariate normal distribution as approximate posterior.

```

1:  $\mathcal{F} : \{\theta^{(0)}\} \leftarrow \mathcal{X}(\cdot)$        $\triangleright$  init w. strategy  $\mathcal{X}$ 
2:  $q : \{\mu_i^{(0)}, \Sigma_i^{(0)}\} \leftarrow \{\mathcal{U}(-\epsilon, \epsilon), I_\epsilon\}$        $\triangleright$  init w.  $\epsilon \approx 0$ 
3: repeat:
4:    $[z] \sim q(z|x_i; \mu_i^{(t)}, \Sigma_i^{(t)})$        $\triangleright$  Monte-Carlo sampling
5:    $[p(z|x_i, \theta^{(t)})] = \mathcal{N}(\mathcal{F}([z], \theta^{(t)}); x_i, \Lambda_i)$        $\triangleright$  Eq. 5
6:    $\{\theta, \mu_i, \Sigma_i\}^{(t+1)} \leftarrow \text{grad\_step}_{\theta, \mu_i, \Sigma_i} \left( \mathcal{V}(q^{(t)}, \theta^{(t)}|x_i) \right)$ 
7:    $t \leftarrow t + 1$ 
8: until convergence on  $\mathcal{V}$ 

```

from a family of known simpler distributions where sampling can be easily done. Depending on the complexity of the data and the posterior in Equation 5, the choice for the approximate posterior may change. For a chosen q , the following variational lower bound is maximized after sampling is done from posterior p .

$$\underset{\phi}{\operatorname{argmax}} \mathcal{V}(q_\phi, \theta^*|x_i) \quad (7)$$

To maximize the above equation, the Expectation Maximization (EM) algorithm can be employed to learn ϕ in a such a way that samples from $p(z|x_i, \Lambda_i)$ are reasonably generated by the approximate posterior. The output of the inference is $q_\phi(z|x_i)$ for a given data point x_i .

4.1.2. TRAINING

In the previous section, we assumed that the decoder $\mathcal{F}(z|\theta^*)$ with parameters θ^* was provided. However, in practice, θ needs to be learned during training process. Maximizing variational lower bound \mathcal{V} is usually not tractable w.r.t θ , hence a gradient ascent approach can be taken. The training procedure of VAD models can be summarized in an iterative framework for maximizing the variational lower bound \mathcal{V} : in the first step, inference is performed as defined in Subsection 4.1.1, hence maximizing the lower bound w.r.t ϕ . Subsequently, the lower bound is maximized w.r.t θ in the second step. These two steps are iteratively taken until no further meaningful improvement in the lower bound is

achieved. The output of training are parameters θ^* of the trained decoder.

4.2. Efficient Inference

For VAD models, inference can be time consuming due to utilizing MCMC sampling methods to sample from the posterior in Equation 5. Even faster sampling methods such as Hamiltonian Monte Carlo (Neal and others, 2011) methods still require a reasonable number of samples to be drawn. Moreover, once sampling is done, an iterative approach is still needed to fit the approximate distribution to the generated samples. One approach to speed up the convergence during inference is constraining the degree of freedom for the approximate posterior. This acts as a regularizer on the input space of the decoder, encouraging it to follow certain desirable properties. Similar to VAE, the approximate posterior can be assumed to be a normal distribution with mean μ_i and a covariance Σ_i :

$$q(z|x_i; \mu_i, \Sigma_i) := \mathcal{N}(z; \mu_i, \Sigma_i) \quad (8)$$

During training, the above approximate posterior regularizes parameters θ of the decoder such that samples from posterior $p(z|x_i, \Lambda_i)$ will have a concentrated density by conforming to a normal distribution. This assumption that inputs to the decoder follow a normal distribution can then be used to modify the inference process: As opposed to performing a random walk to sample from the posterior $p(z|x_i, \Lambda_i)$ and then fitting an approximate posterior q to the sampled points, one can sample from q , use those samples as input to p to evaluate the variational lower bound \mathcal{V} . The variational lower bound is therefore differentiable w.r.t μ_i , hence simple gradient ascent techniques can be used to perform inference. Using this method, during training, the variational lower bound is updated using gradient ascent w.r.t both θ , μ_i and Σ_i . During inference the variational lower bound is updated using gradient ascent w.r.t μ_i and Σ_i only, without the need to sample from posterior $p(z|x_i, \Lambda_i)$. Batch training and inference is therefore easily possible. Algorithms 1 and 2 summarize the inference and training procedure for this implementation of VAD.

5. Experimental Setup

The goal of the experiments in this paper is to establish a comparison between VAD and VAE for generative modeling of partial data. During training, both VAD and VAE use the same posterior in Equation 5 and maximize the same variational lower bound². As common in models with an

²This implementation of VAE (through Equation 5) is similar to a recent state-of-the-art approach in data imputation (Ivanov et al., 2018) which was published during preparation of this paper. Therefore, this baseline is very competitive and according to the authors of the above paper, outperforms existing data imputation techniques such as GAIN (Yoon et al., 2018).

encoder, missing values are imputed by zeros before being used as input to encoder. VAD models use the efficient inference described in Subsection 4.2.

In this paper we perform experiments using several challenging datasets, most of which are multimodal (heterogeneous). Multimodal datasets provide a suitable test bench for generative modeling from partial data due to two reasons: 1) Multimodal datasets usually exhibit complex relations between modalities (cross-modal complexities), as opposed to homogeneous datasets where dependencies are sometimes simpler (e.g. a missing pixel most likely has similar color to adjacent pixels). Therefore, missingness in multimodal datasets creates challenging experimental conditions. 2) Multimodal phenomena often include natural missingness. In fact, multimodal machine learning strives to learn a phenomena from increasing number of sources, which in turn means increasing chances of missingness since not all sources may be present per each datapoint. Therefore, multimodal datasets can be used to create realistic experimental conditions.

The datasets used for experiments in this paper allow for variety across different factors such as different ranges of missingness, large and small number of modalities, synthetic and natural data, as well as large and small dataset sizes. Specifically, the following tasks and accompanying datasets are used: 1) We first create a synthetic multimodal task where the number of modalities as well as the distribution of each modality are controllable parameters. We create datasets with 10, 20, and 30 modalities. 2) The second task is statistical shape modeling, which is a real-world multi-view computer vision task (Dryden et al., 1998). We use the Menpo (Zafeiriou et al., 2017) dataset for this task. 3) The third experimental task involves modeling multimodal language using text, vision and acoustic modalities (Zadeh et al., 2018). We use CMU-MOSEI (Zadeh et al., 2018) and CMU-MOSI (Zadeh et al., 2016) datasets.

Evaluation procedure in our experiments is as follows. The ground truth train, validation and test data is never used during training, validation or testing of any of the models. However, datasets used in our experiments allow for ground-truth test data to be revealed only for evaluation purposes. In simple terms, this means that while all the models are blind to the ground-truth data at all stages (training, testing and evaluation), they are judged on how well the outputs of the decoder (with inference done only using partial data) are close to the ground truth. We calculate the Mean-Squared Error (MSE) distance between ground truth data and the decoder output. Furthermore, in Appendix A we report MSE for available and missing dimensions to evaluate how well each of the partial data and missing data were approximated.

To establish a range for reasonable performance, we report two measures for each dataset. The first measure is

Dataset	Segment	Model	Missing Ratio (r)								
			0.1	0.2	0.3	0.4	0.5	0.6	0.7	0.8	0.9
Synthetic	Full	VAE	0.0012	0.0014	0.0021	0.0044	0.0060	0.0118	0.0197	0.0447	0.1324
		VAD	0.0009	0.0003	0.0010	0.0019	0.0014	0.0006	0.0041	0.0030	0.0406
	Missing	VAE	0.0022	0.0022	0.0037	0.0060	0.0081	0.0153	0.0241	0.0516	0.1438
		VAD	0.0013	0.0010	0.0032	0.0041	0.0024	0.0009	0.0059	0.0037	0.0450
	Partial	VAE	0.0004	0.0005	0.0011	0.0020	0.0017	0.0028	0.0054	0.0039	0.0091
		VAD	0.0003	0.0001	0.0001	0.00001	0.0001	0.00005	0.00004	0.00002	0.000005

Table 1. Numerical MSE results of experiments on the synthetic multimodal dataset with $K = 2$ modalities (Section 6.1). VAD models show superior performance across various ranges of missing data.

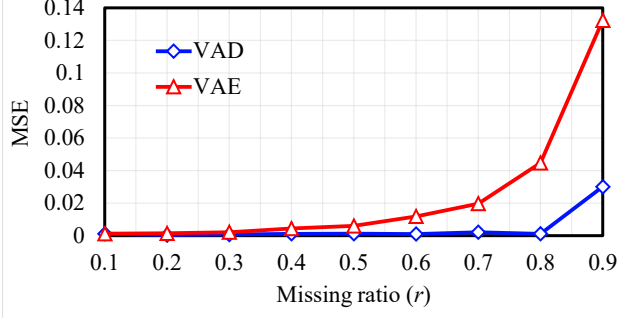


Figure 1. Performance trend for experiments in Section 6.1 over synthetic data $K = 2$.

achieved by training, validation and testing on the ground truth data. This establishes a proxy for best achievable performance under ideal conditions for both VAD and VAE models. The second measure establishes a worst-case performance through a threshold indicating when the models are working worse than predicting the mean for each dimension, regardless of the input. We report these two measure in the body of each experiment to help better understand the differences in model performance.

All the datasets in this paper are available for download and further exploration through [hidden-for-blind-review](#), alongside a generic implementation of VAD. Further information regarding hyperparameter search and implementation details are provided in Appendix B.

6. Experiments

6.1. Synthetic Multimodal Experiments

In the first experiment, we study the case of synthetic multimodal data where the number of modalities as well as missingness pattern are controlled. We define the input multimodal data $\hat{x}_i = [\hat{x}_{i(1)}, \hat{x}_{i(2)}, \hat{x}_{i(3)}, \dots, \hat{x}_{i(K)}]$ for K different modalities. Data for each modality contains independent and dependent dimensions: while information exhibits different nature from one modality to another, modalities are not fully independent.

To generate the synthetic multimodal data, we first generate the independent component of each modality as follows: we randomly initialize 5 independent dimensions for each modality based on univariate distributions: {Normal, Uniform, Beta, Logistic, Gumbel}. Each instance is chosen uniformly at random, and the appropriate parameters are also chosen uniformly at random³. To generate dependent components of each modality, we pick a random subset of other modalities' independent components and combine them with a random subset of independent components of the modality in hand. Operations include weighted multiplication, addition, and activation⁴. Using this method, we generate a dataset containing $N = 50,000$ datapoints with ground-truth dimension $d = 300$, with $K = \{2, 4, 6\}$ modalities.

Once the ground-truth dataset is created using the above formulation, we experiment with a severe case of dimensional missingness: For each \hat{x}_i , we sample a missing pattern $\alpha_i \sim \text{Bernouli}(r); \alpha_i \in \{0, 1\}^{300}$ with missing ratio r ranging from 0.1 to 0.9 with increments of 0.1. This form of α_i essentially allows the data to be randomly missing at each dimension of the ground-truth multimodal input. Table 1 and Figure 1 show the ground truth MSE performance trend between VAD and VAE when $K = 2$. Lowest achieved MSE for $r = 0$ (no missingness) in this dataset is 0.00012 for VAD and 0.00006 for VAE. The performance threshold is 0.54663, indicating the limit beyond which models are performing worse than predicting average of each dimension in ground-truth data. Results for $K = 4$ and $K = 6$ follow similar trend (discussed in Appendix A).

6.2. Statistical Shape Modeling

Statistical shape modeling is a well-known research area in the field of computer vision. This research area deals with multiview data (data coming from different cameras). The goal is to learn a generative model for variations of a particular shape across different camera view points. The shapes are usually described as a cloud of annotated landmarks in

³Exact ranges given in Table 12 in Appendix.

⁴Exact data and generation process are available in [hidden-for-blind-review](#).

Dataset	Segment	Model	Missing Ratio (r)									
			0.1	0.2	0.3	0.4	0.5	0.6	0.7	0.8	0.9	
Menpo	Full	VAE	0.00057	0.00094	0.00119	0.00145	0.00167	0.00196	0.00247	0.00347	0.00693	
		VAD	0.00005	0.00008	0.00017	0.00022	0.00027	0.00036	0.00062	0.00112	0.00357	
	Missing	VAE	0.00084	0.00109	0.00132	0.00156	0.00180	0.00207	0.00258	0.00363	0.00718	
		VAD	0.00018	0.00023	0.00028	0.00036	0.00044	0.00051	0.00077	0.00132	0.00396	
	Partial	VAE	0.00054	0.00090	0.00114	0.00138	0.00154	0.00176	0.00218	0.00282	0.00449	
		VAD	0.00004	0.00001	0.00008	0.00004	0.00002	0.00003	0.00001	0.00003	0.000003	

Table 2. Numerical MSE results from statistical shape modeling experiments in Section 6.2 for Menpo. VAD models show superior performance across various ranges of missing data.

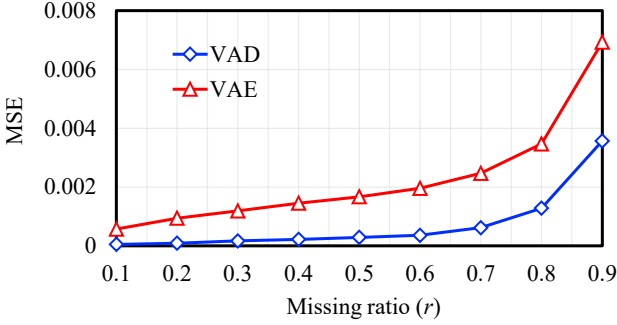


Figure 2. Performance trend for statistical shape modeling experiments in Section 6.2.

2D. Some of these landmarks may be occluded depending on the geometry of the object (self-occlusions) as well as the camera and scene configurations. These occlusions in turn lead to natural data missingness. The dataset of this experiment is the Menpo facial landmarks dataset (Zafeiriou *et al.*, 2017). Menpo contains 13391 facial images with various expressions and poses (or camera positions). Since Menpo dataset has ground truth annotations for 84 landmarks regardless of self-occlusions in the natural image, it allows for creating a real-life ground-truth data for our experiments.

As with the synthetic data, we experiment with missingness distributions $\alpha_i \sim \text{Bernoulli}(r); \alpha_i \in \{0, 1\}^d; d = 84$, where r varies from 0.1 to 0.9 in increments of 0.1. Table 2 and Figure 2 show the ground truth MSE performance trend between VAD and VAE. Lowest achieved MSE for $r = 0$ (no missingness) in this dataset is 0.00002 for VAD and 0.000006 for VAE. The performance threshold is 0.06210, indicating the limit beyond which models are performing worse than predict average of each dimension in ground-truth data.

6.3. Multimodal Language Experiments

Natural language, as developed throughout evolution from cries and imitations to words and gesture, is a multimodal phenomena (Müller, 1866; Langendoen, 1993). In its general form as face-to-face communication, it involves three modalities of text (words), vision (gestures) and acoustic

(sound) (Morency *et al.*, 2011). This multimodal definition of language is a recent trend of study in Natural Language Processing (NLP) research (Zadeh *et al.*, 2018). A challenging area of modeling language as a multimodal phenomena is that instances of communication are scattered across various mediums where language occurs alone (e.g. online reviews or books), alongside acoustics modality (e.g. podcasts) or alongside both visual and acoustic modalities (face-to-face communication). Thus a large dataset of multimodal language spanning across different mediums of communication naturally exhibits missing data.

In this section, we choose the CMU-MOSEI (Zadeh *et al.*, 2018) and CMU-MOSI (Zadeh *et al.*, 2016) datasets, which are targeted by studies of multimodal language (Liang *et al.*, 2018; Poria *et al.*, 2017). Both datasets consist of sentences from online YouTube monologue videos. CMU-MOSEI consists of 23,500 sentences and CMU-MOSI consists of 2199 sentences.

For text modality, the datasets contain GloVe word embeddings (Pennington *et al.*, 2014) trained on 840 billion tokens from the Common Crawl dataset. The word vectors are aligned with the transcript (Yuan and Liberman, 2008). For visual modality, the datasets contain facial action units, facial landmarks, and head pose information. For acoustic modality, the datasets contain high and low-level descriptors including 12 Mel-frequency cepstral coefficients, pitch tracking and voiced/unvoiced segmenting features, glottal source parameters, peak slope parameters and maxima dispersion quotients (Degottex *et al.*, 2014). We use expected multimodal context for each sentence, similar to unordered compositional approaches in NLP (Iyyer *et al.*, 2015).

To simulate the missingness due to different means of communication, we randomly drop entire modalities from each datapoint. The process consists of two steps: first, a Bernoulli trial with probability of success r is run for each datapoint. Then, if the trial is successful, a non-empty proper subset of modalities is chosen uniformly at random to be dropped. For example, for the i -th datapoint, the audio and visual modalities may be dropped, leaving only text. To experiment with different ranges of missingness, we change the missingness ratio r from 0.1 to 0.9 with in-

Dataset	Segment	Model	Missing Ratio (r)								
			0.1	0.2	0.3	0.4	0.5	0.6	0.7	0.8	0.9
MOSI	Full	VAE	0.0020	0.0028	0.0025	0.0030	0.0035	0.0039	0.0044	0.0048	0.0049
		VAD	0.0007	0.0013	0.0014	0.0016	0.0015	0.0025	0.0029	0.0031	0.0033
	Missing	VAE	0.0059	0.0068	0.0057	0.0060	0.0067	0.0059	0.0061	0.0066	0.0059
		VAD	0.0047	0.0068	0.0054	0.0057	0.0064	0.0062	0.0061	0.0062	0.0058
	Partial	VAE	0.0018	0.0021	0.0017	0.0022	0.0022	0.0024	0.0023	0.0021	0.0033
		VAD	0.0007	0.0005	0.0007	0.0005	0.0005	0.0007	0.0006	0.0006	0.0005

Table 3. Numerical MSE results of experiments on the MOSI dataset in Section 6.3. VAD models show superior performance across various ranges of missing data.

Dataset	Segment	Model	Missing Ratio (r)								
			0.1	0.2	0.3	0.4	0.5	0.6	0.7	0.8	0.9
MOSEI	Full	VAE	0.00275	0.00552	0.00794	0.00962	0.01232	0.01485	0.01590	0.01801	0.02002
		VAD	0.00072	0.00185	0.00274	0.00331	0.00537	0.00474	0.00559	0.00742	0.01063
	Missing	VAE	3.7176	4.2242	4.6522	4.2153	4.7448	4.6900	4.5024	4.3818	4.2123
		VAD	1.3868	1.7578	1.7062	1.5995	2.1956	1.5746	1.6123	1.8775	2.3084
	Partial	VAE	0.0108	0.0105	0.0102	0.0107	0.0105	0.0092	0.0093	0.0098	0.0076
		VAD	0.0017	0.0011	0.0009	0.0011	0.0018	0.0015	0.0010	0.0015	0.0007

Table 4. Numerical MSE results of experiments on the MOSEI dataset in Section 6.3. VAD models show superior performance across various ranges of missing data.

crements of 0.1. Tables 4, 3 and Figure 1 show the ground truth MSE performance trend between VAD and VAE for CMU-MOSEI and CMU-MOSI datasets. Lowest achieved MSE for $r = 0$ (no missingness) in CMU-MOSEI and CMU-MOSI are respectively 0.01975, 0.000546 for VAD and 0.0041, 0.0011 for VAE. The performance threshold is 0.00674 and 0.05835 for CMU-MOSI and CMU-MOSEI, indicating the limit beyond which models are performing worse than predict average of each dimension in ground-truth data.

7. Discussion

Figures 1, 3, and 2 show a consistent trend of superior performance for VAD models: As the missing ratio increases, the gap between VAD and VAE models widens. The gap in performance can be quite large: for example, in Figure 2, VAD on $r = 0.5$ performs better than VAE at all missingness ratios.

Since the only major difference between the architecture of the two models is the encoder, the large gap between the performance of the two models indicates that encoders fail to marginalize the effect of missing data. Unsurprisingly, input volatility caused by missing data is the main reason behind this, as we empirically observe that increasing the missing ratio significantly reduces the performance of VAE.

So far, we only studied the case where train and test time missingness follow similar missingness ratios. However, in naturalistic scenarios this assumption may not necessarily be true. For example, consider a generative model trained on inputs coming from sensors spread across a distributed wireless sensor network. During test time, an arbitrary number

of sensors may not be able to respond in time due to network latency or sensor failure, creating potential adversarial inputs.

We perform an experiment where models are trained on ground-truth train data \hat{x} , however, during testing, information can be arbitrarily missing. After training on ground-truth data, we change the missingness ratio r during test time from 0.1 to 0.9 following Bernouli (r) (similar to Subsection 6.1). Evaluation remains the same as before, on ground-truth test data. Figure 4 shows the trend of performance between VAD and VAE models for Menpo and Synthetic $K = 2$ datasets.

We observe that even small amount of test-time missingness can cause severe instability for VAE, while VAD models remain consistent. In fact, their performance is almost identical to the case where they are trained on the same missingness ratio as test-time (shown with solid lines as borrowed from Figures 1 and 2). This shows superior stability in the face of test-time adversarial conditions. The opposite experiment, where during training, data with missingness is used and during testing ground-truth data is used is reported in Appendix A; however, this case is less likely to happen in naturalistic scenarios.

8. Conclusion

In this paper we studied an alternate implementation of AVEB algorithm, called Variational Auto-Decoder (VAD). We outlined a generic inference and training framework based on Variational Bayes and Markov Chain Monte Carlo methods. We presented an efficient inference process without the need for MCMC sampling from the decoder. Our

Dataset	Model	Missing Ratio (r)								
		0.1	0.2	0.3	0.4	0.5	0.6	0.7	0.8	0.9
Synthetic	VAE	0.05188	0.11393	0.18117	0.25699	0.34486	0.43963	0.54251	0.64795	0.76105
	VAD	0.00024	0.00036	0.00049	0.00067	0.00091	0.00121	0.00173	0.00347	0.02193
Menpo	VAE	0.01480	0.03164	0.05048	0.07250	0.09784	0.12638	0.16090	0.19923	0.25049
	VAD	0.00019	0.00038	0.00069	0.00113	0.00169	0.00242	0.00339	0.00535	0.01315

Table 5. Numerical results of test-time adversarial experiments where training is done on ground-truth train data and testing is done on data with missingness, following the ratio r for Synthetic $K = 10$ and Menpo datasets. VAD models are more robust than VAE models to this form of adversarial condition.

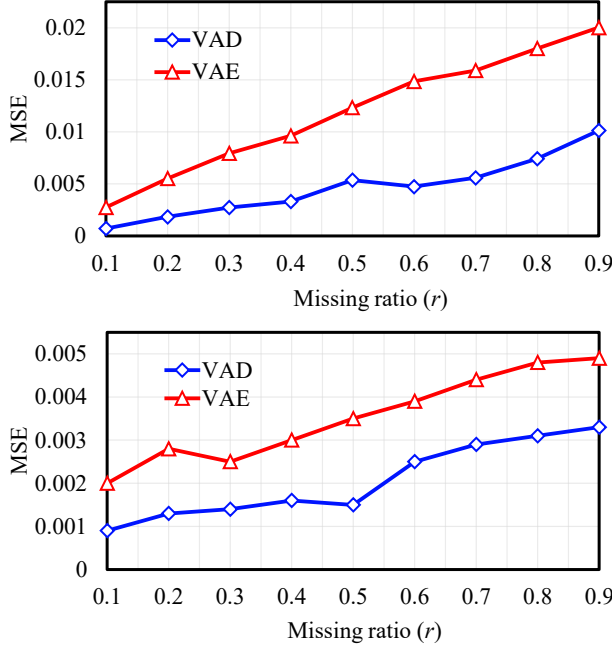


Figure 3. Performance trend for multimodal language experiments in Section 6.3 over CMU-MOSEI (top) and CMU-MOSI (bottom) datasets.

experimental results showed superior performance of VAD across multiple datasets with various missingness ratios. Aside superior performance, VAD does not require similar missingness during training and testing which is an appeal for real-world applications.

References

Gilles Degottex, John Kane, Thomas Drugman, Tuomo Raitio, and Stefan Scherer. Covarep: A collaborative voice analysis repository for speech technologies. In *Acoustics, Speech and Signal Processing (ICASSP), 2014 IEEE International Conference on*, pages 960–964. IEEE, 2014.

Ian L Dryden, Kanti V Mardia, et al. Statistical shape analysis, 1998.

Oleg Ivanov, Michael Figurnov, and Dmitry Vetrov. Variational autoencoder with arbitrary conditioning. 2018.

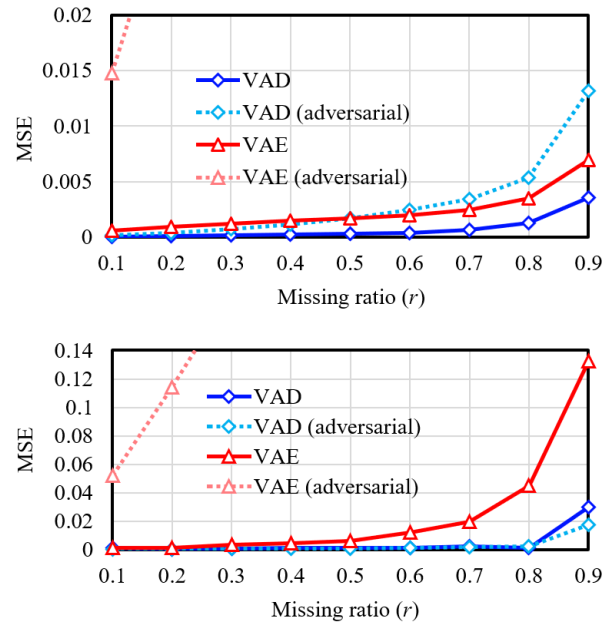


Figure 4. Performance trend for adversarial conditions described in Section 7 where training is done on ground-truth data and testing can undergo missingness (dotted lines) for Menpo (top) and Synthetic $K = 2$ (bottom). We also compare to models trained and tested on similar missing ratios (solid lines).

Mohit Iyyer, Varun Manjunatha, Jordan Boyd-Graber, and Hal Daumé III. Deep unordered composition rivals syntactic methods for text classification. In *Proceedings of the 53rd Annual Meeting of the Association for Computational Linguistics and the 7th International Joint Conference on Natural Language Processing (Volume 1: Long Papers)*, volume 1, pages 1681–1691, 2015.

Diederik P Kingma and Jimmy Ba. Adam: A method for stochastic optimization. *arXiv preprint arXiv:1412.6980*, 2014.

Diederik P Kingma and Max Welling. Auto-encoding variational bayes. *arXiv preprint arXiv:1312.6114*, 2013.

D Terence Langendoen. Natural language and universal grammar, 1993.

Paul Pu Liang, Ziyin Liu, Amir Zadeh, and Louis-Philippe Morency. Multimodal language analysis with recurrent multistage fusion. *arXiv preprint arXiv:1808.03920*, 2018.

Nicholas Metropolis, Arianna W Rosenbluth, Marshall N Rosenbluth, Augusta H Teller, and Edward Teller. Equation of state calculations by fast computing machines. *The journal of chemical physics*, 21(6):1087–1092, 1953.

Louis-Philippe Morency, Rada Mihalcea, and Payal Doshi. Towards multimodal sentiment analysis: Harvesting opinions from the web. In *Proceedings of the 13th international conference on multimodal interfaces*, pages 169–176. ACM, 2011.

Friedrich Max Müller. *Lectures on the science of language: Delivered at the Royal Institution of Great Britain in April, May, & June 1861*, volume 1. Longmans, Green, 1866.

Radford M Neal et al. Mcmc using hamiltonian dynamics. *Handbook of markov chain monte carlo*, 2(11):2, 2011.

Jeffrey Pennington, Richard Socher, and Christopher D Manning. Glove: Global vectors for word representation. 2014.

Soujanya Poria, Erik Cambria, Devamanyu Hazarika, Navonil Mazumder, Amir Zadeh, and Louis-Philippe Morency. Multi-level multiple attentions for contextual multimodal sentiment analysis. In *2017 IEEE International Conference on Data Mining (ICDM)*, pages 1033–1038. IEEE, 2017.

Jinsung Yoon, James Jordon, and Mihaela van der Schaar. Gain: Missing data imputation using generative adversarial nets. *arXiv preprint arXiv:1806.02920*, 2018.

Jiahong Yuan and Mark Liberman. Speaker identification on the scotus corpus. *Journal of the Acoustical Society of America*, 2008.

Amir Zadeh, Rowan Zellers, Eli Pincus, and Louis-Philippe Morency. Multimodal sentiment intensity analysis in videos: Facial gestures and verbal messages. *IEEE Intelligent Systems*, 31(6):82–88, 2016.

AmirAli Bagher Zadeh, Paul Pu Liang, Soujanya Poria, Erik Cambria, and Louis-Philippe Morency. Multimodal language analysis in the wild: Cmu-mosei dataset and interpretable dynamic fusion graph. In *Proceedings of the 56th Annual Meeting of the Association for Computational Linguistics (Volume 1: Long Papers)*, volume 1, pages 2236–2246, 2018.

Stefanos Zafeiriou, George Trigeorgis, Grigoris Chrysos, Jiankang Deng, and Jie Shen. The menpo facial landmark localisation challenge: A step towards the solution. In *The IEEE Conference on Computer Vision and Pattern Recognition (CVPR) Workshops*, volume 1, page 2, 2017.

Appendices

A. Numerical Results

This appendix presents the detailed numerical results for the experiments in this paper. The results are reported on the test set of the studied datasets. For VAD and VAE models, numerical MSE evaluations are reported on the ground-truth data, missing data and partial data. All models only use partial data during test-time inference.

For experiments in Subsection 6.1, we report the numerical results in Table 1 for $K = 2$, Table 6 for $K = 4$ and Table 7 for $K = 6$. Lowest achieved MSE for $r = 0$ in $K = 4$ dataset is 0.00030 for VAD and 0.00017 for VAE. Lowest achieved MSE for $r = 0$ in $K = 6$ dataset is 0.00018 for VAD and 0.00014 for VAE.

For experiments in Subsection 6.2, we report the numerical results in Table 2.

For experiments in Subsection 6.3, we report the results in Table 3 for CMU-MOSI and 4 for CMU-MOSEI.

For experiments regarding adversarial test-time conditions, Table 5 shows the performance when training is done on fully observed data and testing is done on partial test data. The opposite is presented in the Table 9, where training is done on partial data, and testing is done on ground-truth test data. Unlike previous experiments, this is the only case where testing is directly done on ground-truth data.

We also present numerical results for comparison between SGD and Adam for learning parameters μ_i of the Gaussian approximate posterior q . The choice of optimization method directly impacts the convergence of the VAD models. This is in part due to the high degree of freedom of the parameters of the approximate posterior. Table 10 shows the comparison between VAD models which use SGD or Adam during training and inference.

Similar to the missingness method and ratio used in Section 6.1, we also perform experiments with MNIST. Figure 5 shows the performance trend across various missingness ratios and Table 8 presents numerical comparisons. VAD still outperforms VAE, however, margin is less than complex datasets in the body of the paper.

B. Implementation Remarks

The following subsections describe the implementation remarks for the experiments in this section.

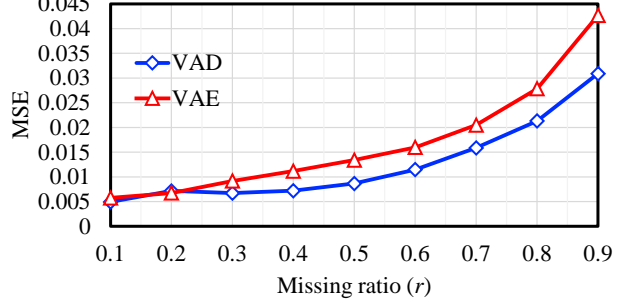


Figure 5. Comparison of models trained on the MNIST dataset.

B.1. Efficient Inference

Sampling from approximate posterior q using efficient inference in VAD was done only with 1 sample. In simple terms, to do the forward pass, we only sample once from q parameterized with μ_i and Σ_i . This, in practice seemed to work reasonably well for reconstruction purposes. However, better generative qualities may be achieved

B.2. Variance Analysis

During inference, both models use an approximate posterior with a learnable variance. However, in practice when using partial data, learning the variance was a very unstable process. VAE models showed very high sensitivity to even small variances, quickly performing similar to projecting the mean in each dimension. We believe combination of noise from imputed values and also the noise added through approximate posterior may cause uncertainties. While VAD models suffered similarly from the same instability during learning the variance, the performance was better than VAE.

Therefore, during our experiments we treated the approximate posterior variance as a hyperparameter. This way results improved substantially. The best performing variance may change depending on the problem and the range of the input space, however, in general we observed that very large variances did not converge well, while small variances did not yield the best results. In practice the variance and performance can form a tradeoff: higher variances show better generative properties, while low variances show better reconstructions.

B.3. VAE Reparameterization Trick

The VAE reparameterization trick can be used to regularize the posterior space to follow certain desirable properties. Since VAD and VAE follow the same framework, the same reparameterization trick can be applied to both. While the focus of this paper is on reconstruction performance, this reparameterization trick can be used similarly to VAE to improve the generative properties of VAD. For further read-

Dataset	Segment	Model	Missing Ratio (r)								
			0.1	0.2	0.3	0.4	0.5	0.6	0.7	0.8	0.9
Synthetic	Full	VAE	0.0069	0.0097	0.0158	0.0186	0.0285	0.0417	0.0896	0.1084	0.2657
		VAD	0.0052	0.0020	0.0090	0.0016	0.0062	0.0085	0.0489	0.0610	0.2052
	Missing	VAE	0.0111	0.0167	0.0253	0.0271	0.0328	0.0485	0.1104	0.1282	0.2907
		VAD	0.0090	0.0081	0.0181	0.0030	0.0111	0.0140	0.0698	0.0754	0.2274
	Partial	VAE	0.0011	0.0012	0.0016	0.0036	0.0027	0.0036	0.0060	0.0054	0.0094
		VAD	0.0001	0.0001	0.0002	0.00002	0.0004	0.0002	0.0001	0.0002	0.000006

Table 6. Numerical MSE results of experiments on the synthetic multimodal dataset with $K = 4$ modalities (Section 6.1). VAD models show superior performance across various ranges of missing data.

Dataset	Segment	Model	Missing Ratio (r)								
			0.1	0.2	0.3	0.4	0.5	0.6	0.7	0.8	0.9
Synthetic	Full	VAE	0.0032	0.0047	0.0059	0.0162	0.0150	0.0242	0.0564	0.0910	0.1900
		VAD	0.0023	0.0011	0.0018	0.0040	0.0032	0.0039	0.0182	0.0436	0.1292
	Missing	VAE	0.0110	0.0129	0.0130	0.0237	0.0240	0.0349	0.0607	0.1045	0.2076
		VAD	0.0140	0.0032	0.0030	0.0069	0.0050	0.0063	0.0259	0.0545	0.1434
	Partial	VAE	0.0012	0.0011	0.0015	0.0029	0.0025	0.0032	0.0052	0.0037	0.0063
		VAD	0.0003	0.0001	0.0001	0.00002	0.0001	0.0002	0.0002	0.00003	0.000003

Table 7. Numerical MSE results of experiments on the synthetic multimodal dataset with $K = 6$ modalities (Section 6.1). VAD models show superior performance across various ranges of missing data.

ings on this reparametrization trick, please refer to Auto-Encoding Variational Bayes paper (Kingma and Welling, 2013).

B.4. Experimental Methodology

Here we detail the hyperparameter space used for the experiments. Where possible, we tried to establish a fair comparison between the VAD and VAE models by using similar hyperparameters, however both models underwent substantial grid search. We varied three main hyperparameters: the dimensionality of the posterior space d_z , the number of feedforward hidden layers in the decoder \mathcal{F} and the encoder (encoder only for VAE), and the number of hidden units in each hidden layer. A summary is shown in Table 11.

During inference of VAD models, we simply stopped once the model reached a plateau. Since VAD models have a high degree of freedom for approximate posterior q , we observed that it is crucial to use Adam (Kingma and Ba, 2014) for learning the mean of the approximate distribution (Table 10 shows the comparison between SGD and Adam). For both models, learning rates of $10^{\{-2, -3\}}$ for the latent variables and hidden units were used. When running the SGD experiments, learning rates of $10^{\{-1, -2\}}$ were experimented with instead.

To ensure reliability of results in this paper, for both VAD and VAE models, the hyperparameter state space was explored using 20 NVIDIA 1080-Ti GPUs over 2 months in total for all experiments.

Dataset	Segment	Model	Missing Ratio (r)								
			0.1	0.2	0.3	0.4	0.5	0.6	0.7	0.8	0.9
MNIST	Full	VAE	0.00575	0.00674	0.00917	0.01118	0.01341	0.01597	0.02049	0.02783	0.04267
		VAD	0.00495	0.00717	0.00672	0.00721	0.00866	0.01147	0.01588	0.02132	0.03089
	Missing	VAE	0.00963	0.01101	0.01270	0.01461	0.01687	0.01909	0.02327	0.02998	0.04403
		VAD	0.00852	0.01057	0.01049	0.01151	0.01318	0.01474	0.02102	0.02344	0.03370
	Partial	VAE	0.00531	0.00491	0.00749	0.00797	0.00182	0.00922	0.00903	0.00245	0.00534
		VAD	0.00455	0.00628	0.00510	0.00432	0.00413	0.00527	0.00387	0.00320	0.00247

Table 8. Numerical MSE results of experiments on the MNIST dataset. VAD models show superior performance across various ranges of missing data.

Dataset	Model	Missing Ratio (r)								
		0.1	0.2	0.3	0.4	0.5	0.6	0.7	0.8	0.9
Synthetic	VAE	0.00025	0.00025	0.00072	0.00200	0.00152	0.00522	0.00860	0.01727	0.12432
	VAD	0.00030	0.00054	0.00048	0.00020	0.00052	0.00061	0.00043	0.00153	0.00149

Table 9. Numerical results of test-time adversarial experiments where training is done on train data with missingness ratio r and testing is done on ground-truth test data for Synthetic $K = 10$ dataset. VAD models show superior performance compared to VAE models in this adversarial setup.

Dataset	Model	Missing Ratio (r)								
		0.1	0.2	0.3	0.4	0.5	0.6	0.7	0.8	0.9
Synthetic	VAD (SGD)	0.0094	0.0101	0.0146	0.0147	0.0054	0.0604	0.0114	0.0340	0.1009
	VAD (Adam)	0.0012	0.0003	0.0007	0.0011	0.0012	0.0010	0.0021	0.0011	0.0301

Table 10. Numerical MSE results of experiments on the synthetic multimodal dataset with $K = 10$ modalities (Section 6.1), trained with SGD and Adam. VAD models show superior performance when using Adam for training and inference.

Hyperparameter	Group	Values
# of latent variables	A	25, 50, 100
	B	50, 100, 200
# of hidden units per layer	A	50, 100, 200
	B	100, 200, 400
# of hidden layers	A, B	2, 4, 6
LR of hidden units and latent variables	A, B	$10^{-2}, 10^{-3}$

Table 11. Hyperparameters used for the experiments on VAD and VAE across different datasets. Group B refers to MNIST, while group A refers to all other datasets (MOSI/MOSEI, Menpo, synthetic data).

Distribution	Parameter	Range of values
Normal(μ, σ)	μ	$[-1, 1]$
	σ	$(0, 2]$
Uniform(a, b)	a	$[-2, 2]$
	b	$[a, 2]$
Beta(α, β)	α	$[0, 3]$
	β	$[0, 3]$
Logistic(μ, s)	μ	$[-1, 1]$
	s	$(0, 2]$
Gumbel(μ, β)	μ	$[-1, 1]$
	β	$(0, 2]$

Table 12. Parameters used during generation of synthetic multimodal data.